Optical characteristics of a deformable-mirror spatial light modulator

Don A. Gregory

U.S. Army Missile Command, Redstone Arsenal, Alabama 35898-5248

Richard D. Juday

Johnson Space Center, NASA, Houston, Texas 77058

Jeffrey Sampsell, Richard Gale, and R. W. Cohn

Texas Instruments, Dallas, Texas 75266

Stanley E. Monroe, Jr.

Lockheed/EMSCO, Houston, Texas 77058

Received July 6, 1987; accepted September 13, 1987

Some of the optical characteristics of a recently developed solid-state deformable-mirror spatial light modulator have been investigated. The device is composed of an array of 128 × 128 pixels, with each pixel consisting of four hinged reflective rectangular surfaces. Modulation at video frame rates has been achieved, providing real-time displays in coherent light, which may be useful for a variety of optical processing and computing applications.

The deformable-mirror device (DMD) described in this Letter is a monolithic, line-addressed device capable of megahertz pixel-rate operation. Line addressing and monolithic construction offer greater system simplicity than many other spatial light modulators (SLM's), requiring no external interconnections between the light-modulating elements and the addressing circuitry. These two functions are packed into an area only slightly larger than the modulating elements themselves. The DMD is faster than most SLM's and exceeds common liquid-crystal display speeds by orders of magnitude.[1]

A cutaway drawing of a portion of the DMD is shown in Fig. 1. Each element consists of four cantilever-beam deformable mirrors. The elements are fabricated on 2-mil (51-μm) centers, and each of the four mirrors is approximately 0.5 mil (12.7 μm) square. Underneath the array of deformable mirrors is an array of electrodes connected to the floating sources of similarly arrayed metal-oxide semiconductor (MOS) transistors. The role of the addressing circuitry is to drive each electrode to a voltage corresponding to the appropriate video analog level. Thus each set of four deformable mirrors and their underlying electrode form an air-gap capacitor, typically 2 to 3 μm wide. The electrostatic attraction between the capacitor plates causes the deformable mirror to be deflected downward. It is this mirror deflection that is used to modulate light.[2]

The address circuitry is capable of line-at-a-time addressing of the 128 × 128 element array from a single analog input of as great as a 20-MHz data rate. The three major components of the addressing circuitry are (1) a charge-coupled serial-to-parallel analog data converter, (2) 128 high-performance analog driver amplifiers, and (3) a 7-line-to-128-line digital demultiplexer. The analog data input is divided into two data streams, one feeding the drain driver amplifiers on even-numbered array columns and the other feeding the driver amplifiers on odd-numbered columns. Each amplifier channel occupies twice the width of one DMD column because of the relatively large number of transistors in each amplifier. The gate decoder for the 128 × 128 element array has seven inputs to permit selection of one of 128 possible rows of the array in random order. The gate decoder outputs are connected to gates of the MOS transistor array, and drain driver amplifiers are connected to the drains of the array. The 7-bit digital code input to the gate decoder determines which of the 128 rows of the DMD array is to have its gate selected. The sampled

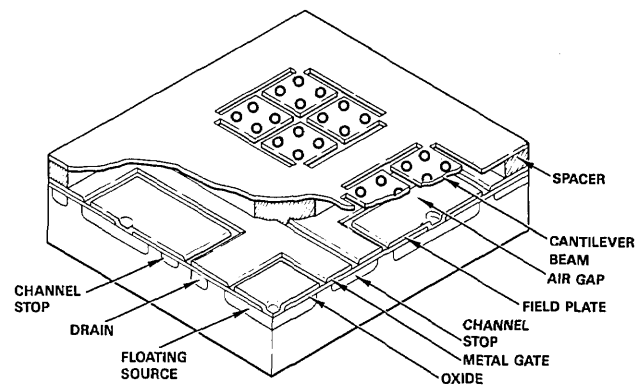

Fig. 1. Cantilever-beam deformable-mirror device spatial light modulator.

0146-9592/88/010010-03$2.00/0

analog data input is propagated down the charge-coupled device (CCD) shift register in the form of charge packets. When the last shift is complete, the charge packets are parallel transferred to charge-to-voltage converters at the input of each operational drain-driver amplifier. An analog voltage proportional to the charge packet in the CCD is then set on each column of the DMD array for the row selected by the gate decoder. The line of data is thereby stored on the floating source capacitors, of which the mirrors form one electrode. The voltage set on the floating source determines the amount of deflection of the overlying mirror.

The structure is built up in layers, using standard MOS processing and photolithography. The active flap is supported by a spacer layer, which performs the additional task of making the underlying addressing circuitry planar, thereby providing a smooth surface upon which to build the metal mirror. The cantilever-flap design also utilizes a dual-thickness process that permits independent control of the mechanical properties of the hinge area and the bulk or mirror area. After the spacer material (a polymer) is spun on and baked, a thin layer of metal is applied. A layer of SiO_2 is then deposited and patterned as a mask for each hinge. A thicker layer of metal is then sputtered on, and the mirror pattern is applied. When this pattern is etched, both thick and thin metals are etched, except where the thin metal is protected by the oxide hinge mask. In this way the hinge area remains thin and flexible, while the majority of the flap can be made robust and stress resistant. Finally, the spacer layer is selectively removed by an isotropic plasma etch procedure to delineate the pixel. The oxide hinge mask is removed during the spacer etch.

Figure 2 demonstrates the cantilever-mirror quality achieved. Interferograms were taken of test devices consisting of individual deflecting elements. Note that each pixel of the DMD consists of four of these deflecting elements. The holes present in each mirror are access holes to facilitate undercutting during the plasma etch of the spacer. The interferograms were taken with 540-nm illumination, so the deflection of approximately two fringes across the 0.7-mil diagonal corresponds to about 1.8 deg. Typical deflection potentials ranged from 3 to 12 V.

There are several problems in relating a DMD model to the data presented, which is a sampling of the visualized intensity variations caused by the DMD in response to real-time activation by a television video signal. The general approach taken in modeling DMD's was to calculate the diffraction pattern for a single pixel, composed of four flaps, and then convolve the result with impulses on a Cartesian grid. It is implicit in this modeling technique that all pixels are identical in their activity. Experiments performed on DMD's have shown that this is patently not the case. In addition to the assumption that all pixels are identical, there were other acknowledged shortcomings in the models. In particular, the physical optics model of diffraction was employed, and the four holes per leaflet were ignored. This approach is deeply in question in that the fundamental diffracting element is only of the order of 20 (visible) wavelengths. The

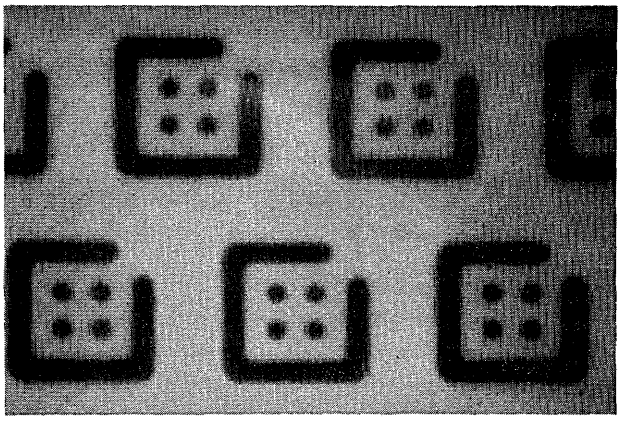

(a) UNDEFLECTED BEAMS

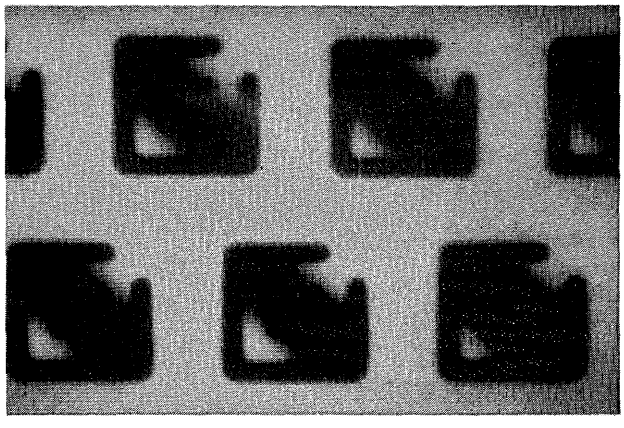

(b) DEFLECTED BEAMS

Fig. 2. Interferograms of (a) undeflected pixels and (b) deflected pixels from a test sample deformable-mirror device.

holes compose a likely nonnegligible fraction of the area of a leaflet. Approximations were necessary in order to solve the diffraction problem with computationally tractable geometry. Altogether, it has been recognized within the program that the modeling of the diffraction has not been entirely accurate. An adaptive method to account for the device's exhibited behavior is already being considered.[3] One significant result of the modeling attempts, however, was the discovery of the origin of the experimentally observed activity in the directions at 45 deg to the Cartesian axes of the DMD, i.e., off axis and in higher orders. It was found that the inclusion of a small randomly distributed initial pixel deflection, which represents a manufacturing nonuniformity, could predict the experimentally observed activity in the four quadrants of the Fourier-transform plane.

Two aspects of the optical activity of the DMD were investigated experimentally: Fourier-plane modulation and imaging using a schlieren-type arrangement.[4] Fourier-plane experimentation addresses the questions of how much light is available for optical processing and which diffraction orders are the most active. The schlieren system permits a measurement of the contrast ratio in the images produced by the DMD.

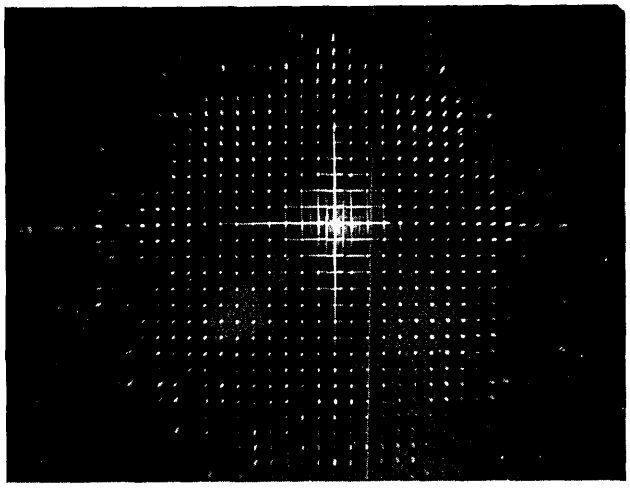

Fig. 3. Intensity distribution in the Fourier-transform plane for a deformable-mirror spatial light modulator.

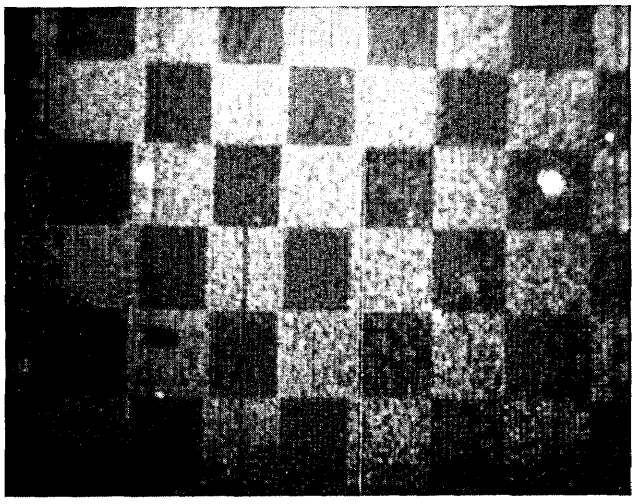

Fig. 4. Photograph of the schlieren display of a DMD driven by a checkerboard scene.

Illumination was provided by a 10-mW (nominal) He–Ne laser. The laser output was filtered, expanded, and recollimated to a 50-mm diameter. A coated pellicle beam splitter was used to provide normal incidence at the DMD. Maximum incident power density at the DMD was 14.3 $\mu W/cm^2$. Light reflected from the DMD and the beam splitter was then collected by the transform lens. A 500-nm focal-length, $f/7.9$ coated doublet was used for the Fourier-plane observations, providing a 6.6-mm separation between diffraction orders. A high-resolution (585 vertical pixels × 488 horizontal pixels, interlaced) 11-mm-diagonal CCD imager was placed one focal length away from the transform lens and was used to record results on video tape.

Two measurements were made to estimate usable modulation in the Fourier-transform plane. The first measurement involved the full deflection of all pixels, compared with no deflection of any of the pixels. This corresponds to an alternating black and then white screen. Diffraction order ($x = 4$, $y = 4$) showed a reasonable white-to-black intensity ratio of about 10:1 as well as being one of the brightest active orders. The second test scene was composed of alternating horizontal and vertical Nyquist spatial-frequency bars (every other row/column deflected). The greatest intensity ratio was again observed in the (4, 4) order. A photograph of the intensity distribution in the Fourier-transform plane is given in Fig. 3 for a DMD having no input signal. Nonuniform defection of the pixels across the device is responsible for the activity shown in the four quadrants.

A schlieren optical system was used to observe the modulation in an image plane. The system was composed of a 160-mm focal-length ($f/1.5$) singlet lens, which provided a separation between fundamental diffraction orders of approximately 2.5 mm. Two types of stop were used in the transform plane: a cross-shaped stop, which could be positioned to block the $x = 0$ and the $y = 0$ orders, and an adjustable rectangular aperture, which could be positioned to block everything except the orders contained in a chosen rectangle. The light was then recollimated with a 155-mm focal-length ($f/1.8$) lens and imaged onto the CCD array. In all cases, neutral-density filters were used to prevent saturation of the CCD array.

Several different inputs were used with the schlieren system. A computer was used to generate various patterns: horizontal and vertical bars of various widths, checkerboards of various sizes, text, etc. A video frame grabber was used in conjunction with the computer to freeze images and display them on the DMD. A special output format CCD camera was used to generate real-time (50-Hz) video, which was then displayed on the DMD. Gray scales were apparent in the frozen-frame and live video displays. The maximum contrast recorded was obtained with a 32 × 32 checkerboard and was measured on the CCD imager output as approximately 2:1. A photograph of a similar scene, taken in He–Ne-laser light, is shown in Fig. 4.

The results presented here are representative only of a brief investigation into some of the optical properties of the deformable-mirror spatial light modulator. The phase-modulating properties of the device have not been properly investigated, and the contrast of schlieren images was found to be rather poor. This is likely due to the overall small percentage active area of the device and the small deflection angle of the pixels. Future devices, under development at this time, will have a larger percentage of active area and should provide higher-contrast images.

References

1. F. T. S. Yu, *Optical Information Processing* (Wiley, New York, 1983), p. 141.
2. D. Pape and L. Hornbeck, Opt. Eng. **22**, 675 (1983).
3. R. E. Juday, "Optimizing a continuously variable filter in a hybrid optical correlator," in *Optics in Computing, Data Processing, and Pattern Recognition* (Institute of Electrical and Electronics Engineers, New York, 1987).
4. A. R. Shulman, *Optical Data Processing* (Wiley, New York, 1970), p. 58.